

Article

Preparation and Characterization of Cu and Al Doped ZnO Thin Films for Solar Cell Applications

Mir Waqas Alam ^{1,*}, Mohd Zahid Ansari ², Muhammad Aamir ³, Mir Waheed-Ur-Rehman ⁴, Nazish Parveen ⁵ and Sajid Ali Ansari ^{1,*}

¹ Department of Physics, College of Science, King Faisal University, Al-Hassa 31982, Saudi Arabia

² School of Materials Science and Engineering, Yeungnam University, Gyeongsan 712749, Korea; zahid.smr@yu.ac.kr

³ Department of Basic Science, Preparatory Year Deanship, King Faisal University, P.O. Box 400, Hofuf, Al-Hassa 31982, Saudi Arabia; msadiq@kfu.edu.sa

⁴ Nanoscience and Nano Technology Unit, Department of Physics, Islamia College of Science and Commerce, Hawal, Srinagar 190001, India; mirwaheed250@gmail.com

⁵ Department of Chemistry, College of Science, King Faisal University, Al-Hassa 31982, Saudi Arabia; nislam@kfu.edu.sa

* Correspondence: wmir@kfu.edu.sa (M.W.A.); sansari@kfu.edu.sa (S.A.A.)

Abstract: The Al- and Cu-doped ZnO nanostructured films in this study were deposited using a sputtering technique. Investigations based on X-ray diffraction, X-ray photoelectron spectroscopy, scanning electron microscopy, Hall effect measurements, and optical transmission spectroscopy was performed to analyze the structural, electrical, and optical characteristics of the prepared Al-ZnO and Cu-ZnO nanostructured films. The analyses show that doping results in enhanced conductivity as well as improved mobility in Al-ZnO and Cu-ZnO films in comparison to pure ZnO films. The Al- and Cu-doped ZnO films exhibited low resistivity ($2.9 \times 10^{-4} \Omega \text{ cm}$ for Al-ZnO and $1.7 \times 10^{-4} \Omega \text{ cm}$ for Cu-ZnO) along with an average transmittance of around 80% in the visible spectrum. Moreover, the optical bandgaps of undoped ZnO, Al-ZnO, and Cu-ZnO nanostructures were observed as 3.3, 3.28, and 3.24 eV, respectively. Finally, solar cells were assembled by employing ZnO nanostructured thin films as photoelectrodes, resulting in efficiencies of 0.492% and 0.559% for Al-ZnO- and Cu-ZnO-based solar cells, respectively.

Keywords: aluminum; copper; doping; solar cells; thin films; zinc oxide



Citation: Alam, M.W.; Ansari, M.Z.; Aamir, M.; Waheed-Ur-Rehman, M.; Parveen, N.; Ansari, S.A. Preparation and Characterization of Cu and Al Doped ZnO Thin Films for Solar Cell Applications. *Crystals* **2022**, *12*, 128. <https://doi.org/10.3390/cryst12020128>

Academic Editor: M. Ajmal Khan

Received: 17 December 2021

Accepted: 14 January 2022

Published: 18 January 2022

Publisher's Note: MDPI stays neutral with regard to jurisdictional claims in published maps and institutional affiliations.



Copyright: © 2022 by the authors. Licensee MDPI, Basel, Switzerland. This article is an open access article distributed under the terms and conditions of the Creative Commons Attribution (CC BY) license (<https://creativecommons.org/licenses/by/4.0/>).

1. Introduction

In the recent past, solar cells have garnered immense interest as the most promising solution to the twin crises of energy shortage and environmental deterioration due to their significant power conversion efficiency (PCE), sustainability, and low cost [1,2]. Nevertheless, the current values of PCE are not satisfactory for the widespread application of solar cells. One of the critical components, which governs the efficiency of a solar cell, is the electrode material. Among the most widely employed metal oxides for photoelectrodes (i.e., zinc oxide (ZnO) and titanium oxide (TiO₂)), ZnO is particularly attractive because of its larger bandgap (~3.37 eV), higher excitonic binding energies (~60 meV) at room temperature, and higher electron mobility than TiO₂. Further, besides being inexpensive and environmentally benign, the electrons of ZnO electrodes demonstrate a longer lifetime in comparison to those of TiO₂ electrodes [3]. As a result, nanostructured ZnO thin films have been extensively employed in gas sensors [4], solar cells [5], and photocatalysts [6]. Doped ZnO is an attractive electrode material for solar cell applications due to enhanced electrical and optical properties, which mainly arise from doping-induced bandgap modification. In the present article, we discuss the fabrication of transparent conducting aluminum- and copper-doped zinc oxide (ZnO) nanostructures, preferably oriented in (101) direction, via

RF sputtering for possible application in solar cells. In addition, the ability to tune the bandgap by simply varying the electron affinity yields further opportunities to enhance the performance of solar cells [7].

Many techniques for obtaining high-quality ZnO nanostructured films have been explored, including chemical vapor deposition (CVD) [8], metal-organic chemical vapor deposition (MOCVD) [9], radiofrequency (RF) sputtering [10], and chemical precipitation [11]. Of these, the RF or DC magnetron sputtering methods offer various merits over the other techniques. The advantages of sputtering include low deposition temperature, fast deposition rates, simple design, cost-effectiveness, and the widespread availability of this deposition technique for growing high-quality films with great uniformity, high packing density, and strong adhesion between the substrate and the film even at fast growth rates [12]. For example, Nomoto et al. [13] and Hirahara et al. [14] deposited high-quality Al-doped ZnO films via RF sputtering at relatively lower temperatures.

Nevertheless, the limited conductivity and low carrier concentration are the most frequently encountered problems with ZnO thin films, which eventually reduce the device efficiency [1]. An important strategy to improve the electron transport in ZnO involves the partial substitution of zinc (Zn) ions with different metal ions [15]. In this regard, the group III elements, such as Al, In, Ga, etc., are extensively explored as n-type dopants in ZnO. Of these, Al is the most widely used dopant to obtain n-type ZnO with high conductivity, high crystal quality, and good optical properties [16]. For instance, Lee et al. [17] reported Al-ZnO thin films deposited over glass substrate via RF sputtering having a low resistivity value of $6.2 \times 10^{-4} \Omega \text{ cm}$ and ~80% average transmittance. Similarly, Wang et al. [18] and Lin et al. [19] prepared Al-ZnO films by simultaneously using non-reactive magnetron sputtering and RF magnetron sputtering. The prepared doped thin films showed resistivity values of 1.4×10^{-3} and $8.43 \times 10^{-3} \Omega \text{ cm}$, respectively. The group of Iwamoto [20] reported greatly enhanced charge transport in Au-decorated ZnO nanorods as photoanode.

Additionally, the elements of group I and group V, such as Li, Na, K, N, P, As, Cu, etc., have also been incorporated as p-type dopants within a ZnO lattice [21]. Of these elements, Cu appears to be the most promising doping species, since it can yield either n-type or p-type doping inside a ZnO matrix, depending upon the synthetic conditions. For instance, Park et al. [22] theoretically predicted p-type behavior for the Cu-doped ZnO. On the contrary, Buchholz et al. [23], in a later study, observed both p- as well as n-type behaviors in Cu-ZnO structures. Incorporating Cu within the structure of ZnO results in modification of absorption as well as other physicochemical properties of ZnO due to the different electronic configurations and the atomic sizes of Zn and Cu. It has been observed that Cu enters the lattice of ZnO via substitution as deep acceptors along with an adjacent oxygen vacancy [24]. Additionally, the surface morphology of the prepared ZnO nanostructures was found to be significantly affected by the addition of Cu. As an example, Raja et al. [25] and Aravind et al. [26] synthesized Cu-doped ZnO nanorods. The authors reported that the introduction of Cu into ZnO nanostructures changed the morphology, resulting in uniformly distributed clusters of elongated nanorods.

Presently, improving the performance of ZnO-based solar cells by incorporating various metal ions has become a major research area. From this perspective, we present the deposition of undoped ZnO, Al-doped ZnO, and Cu-doped ZnO nanostructured films via room temperature radiofrequency (RF) sputtering. The electrical properties of the prepared thin films were measured including resistivity, carrier concentration, and Hall mobility. In addition, the optical characteristics of the obtained films were explored via UV-Vis spectroscopy. Finally, the suitability of both Al-ZnO, and Cu-ZnO nanostructures for use as photoelectrodes in solar cells was analyzed.

2. Materials and Methods

2.1. Materials

Zinc oxide (ZnO; >99%), zinc oxide with aluminum (Al-ZnO; >99%), and zinc oxide with copper (Cu-ZnO; >99%) were acquired from Glenthams Chemicals, Corsham,

UK, whereas the conductive FTO glass was obtained from Pilkington, Minato-ku Tokyo Japan. The $\text{H}_2\text{PtCl}_6 \cdot 6\text{H}_2\text{O}$ and 2-propanol were purchased from Sigma Aldrich, St. Louis, MO, USA.

2.2. Methods

In the present work, the structural investigations of the as-prepared undoped ZnO, Al-doped ZnO, and Cu-doped ZnO nanostructured films were performed using X-ray diffraction (XRD, diffractometer) with Cu $K\alpha$ having a wavelength of 1.5406 Å. The X-ray photoelectron spectroscopic (XPS) investigations were carried out to study the chemical state of Zn, O, Al, and Cu on the surface of ZnO thin films. The XPS instrument was fitted with an Al $K\alpha$ X-ray source maneuvering a 500 nm Rowland circle single crystal silicon (Si) monochromator emitting monochromatic light with at 1486.6 eV and a spread of ~0.85 eV. To record XPS spectral features of all the samples, the C 1s spectrum at 285.0 eV was taken as the reference. Both XRD and XPS investigations were performed in the center of the samples with an area of $20 \times 10 \text{ mm}^2$. The surface morphological features of the obtained films were probed with a scanning electron microscope (SEM). For the morphological characterization, the ZnO, Al-ZnO, and Cu-ZnO thin films were directly deposited onto a conductive FTO substrate. Furthermore, the optical characteristics in the UV-Vis region were examined from the absorbance spectra recorded on a spectrophotometer. The electrical properties including the resistivity, carrier concentration, and Hall mobility of all the samples were analyzed at room temperature by performing Hall effect measurements on a four-point probe. A fixed magnetic field was maintained throughout the Hall effect characterization.

2.3. Solar Cell Fabrication and Characterization

Solar cells were finally fabricated using the as-prepared undoped, Al-doped, and Cu-doped ZnO thin films as photoanodes. To prepare the counter electrode, Pt was deposited on an FTO substrate using a 5 mM solution of $\text{H}_2\text{PtCl}_6 \cdot 6\text{H}_2\text{O}$ in 2-propanol and subsequent annealing at 450 °C. The Pt-coated FTO electrode was situated onto the photoanode, and the edges of the cell were sealed mechanically through the silicone gasket and clamp. A hole was drilled in the counter electrode, through which the electrolyte was fed into the cell. After this, the hole was sealed with the help of tape. Finally, the photocurrent density-voltage (J-V) characteristics of the assembled solar cells were monitored both in the dark as well as illuminated conditions using a simulated solar radiation source with a constant flux of 700 mW/cm^2 obtained through the Autosys DC3500 solar simulator, whereas the current and voltage characteristics were monitored through the Keithley 2400 source meter connected to a computer interface.

2.4. Fabrication of the ZnO, Cu-ZnO, and Al-ZnO Film

The undoped ZnO, Al-ZnO, and Cu-ZnO nanostructured films were deposited over the FTO substrate through a radiofrequency (RF) magnetron sputtering process with a base pressure of $4 \times 10^{-4} \text{ Pa}$ (Figure 1). To grow ZnO films, a high-purity ZnO (99.99%) sputtering target was used, while sintered mixtures of ZnO with Al_2O_3 (>99%) and ZnO with CuO (>99%) were used as targets for depositing Al-ZnO and Cu-ZnO films. Prior to film growth, all substrates were cleaned by ultrasonication in ethanol and acetone. Thereafter, film deposition was performed at constant sputtering power and Ar flow rate of 50 W and 70 sscm, respectively. The substrates were placed at a distance of 12 cm from the target. Prior to film deposition, a pre-sputtering step was introduced, with an RF power of 50 W for 10 min, to remove surface contamination. To maintain film uniformity, the substrates were continuously rotated at ~10 rpm during the film deposition duration.

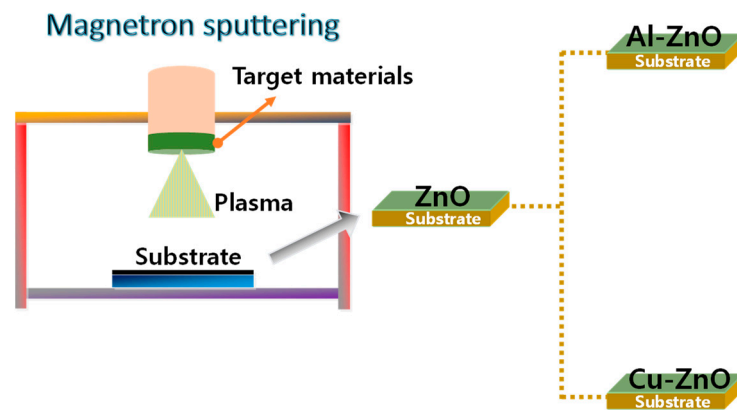


Figure 1. Schematic presentation for the fabrication of the ZnO, Cu-ZnO, and Al-ZnO film.

3. Results and Discussion

Figure 2 depicts the X-ray diffraction (XRD) patterns of as-prepared undoped ZnO, Al-doped ZnO, and Cu-doped ZnO thin films. The strong diffraction peaks in the 2θ range of $36\text{--}36.5^\circ$, associated with the (101) plane, in all the samples, indicate the polycrystalline character of deposited films with a wurtzite structure. The absence of diffraction patterns of aluminum and copper oxides can be explained as follows: (a) the Al and Cu can either substitute for Zn^{2+} in ZnO lattice or enter the ZnO structure [27], (b) these species might be present in amounts lower than the detection limit of the characterizing tool, or (c) these species were segregated in the amorphous form at the grain boundaries [6].

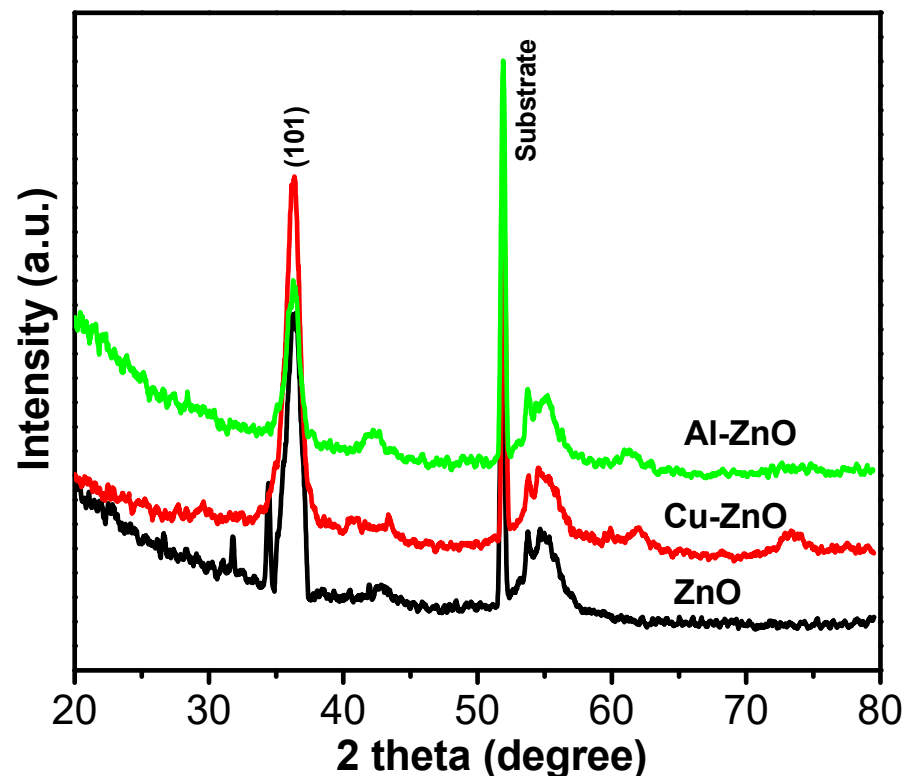


Figure 2. X-ray diffraction (XRD) patterns of as-prepared undoped ZnO, Al-ZnO, and Cu-ZnO thin film samples.

To further confirm the successful injection of Al and Cu species inside the ZnO lattice as interstitial dopants, the oxidation states of Al and Cu in Al-ZnO and Cu-ZnO nanostructures were probed by recording X-ray photoelectron spectroscopy (XPS) spectra for

all the samples, as shown in Figure 3. Figure 3a unveils a highly symmetrical Zn 2p core line, where the binding energies of Zn 2p_{3/2} and Zn 2p_{1/2} remained at 1021.80 ± 0.10 and 1043.80 ± 0.10 eV, respectively. These results confirm that in all the films, the largest majority of Zn atoms existed in the same formal valance state of Zn²⁺ inside the structure of ZnO. The absence of a peak at the binding energy of 1021.50 eV suggests that no metallic Zn was present, and only the oxidized state of Zn existed [28]. Figure 3b–d shows the O 1s, Cu 2p, and Al 2p spectra for the ZnO, Cu–ZnO, and Al–ZnO sample, which also support the presence of copper and aluminum in the ZnO lattices. The absence of any significant changes in the XPS spectrum of ZnO films after doping indicates that the Al and Cu atoms successfully substituted Zn²⁺ sites within the ZnO lattice.

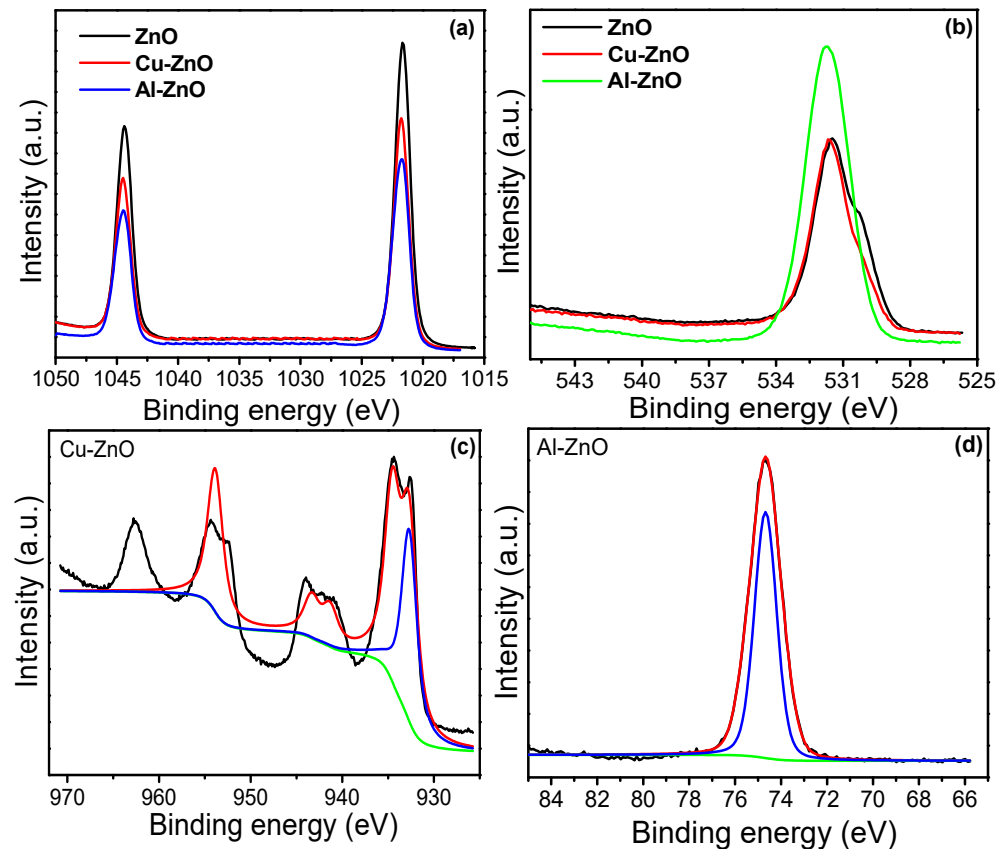


Figure 3. (a) Zn 2p XPS spectra of ZnO, Al–ZnO, and Cu–ZnO; (b) O 1s spectra XPS spectra of ZnO, Al–ZnO, and Cu–ZnO; (c) Cu 2p XPS spectra of Cu–ZnO; and (d) Al 2p XPS spectra of Al–ZnO.

The surface morphologies of the as-developed pure ZnO, Al–ZnO, and Cu–ZnO thin films were examined using scanning electron microscopic (SEM) studies, and the acquired images are shown in Figure 4. The figure evidently reveals uniform surface morphology without the presence of any surface defects, e.g., cracks and voids, mainly due to the low-temperature growth [29]. Furthermore, the SEM micrographs of both Al-doped and Cu-doped ZnO nanostructured films display little or no significant variations in the surface morphology vis-à-vis the undoped ZnO films, indicating the successful incorporation of Cu as a substitutional impurity. These results corroborated the findings of the XRD and XPS investigations. Nonetheless, the Al-doped ZnO films did show a slightly coarse natured surface, which can be attributed to the coalescence of the grain boundaries, as previously reported in the case of Al-doped ZnO films deposited via sputtering [12].

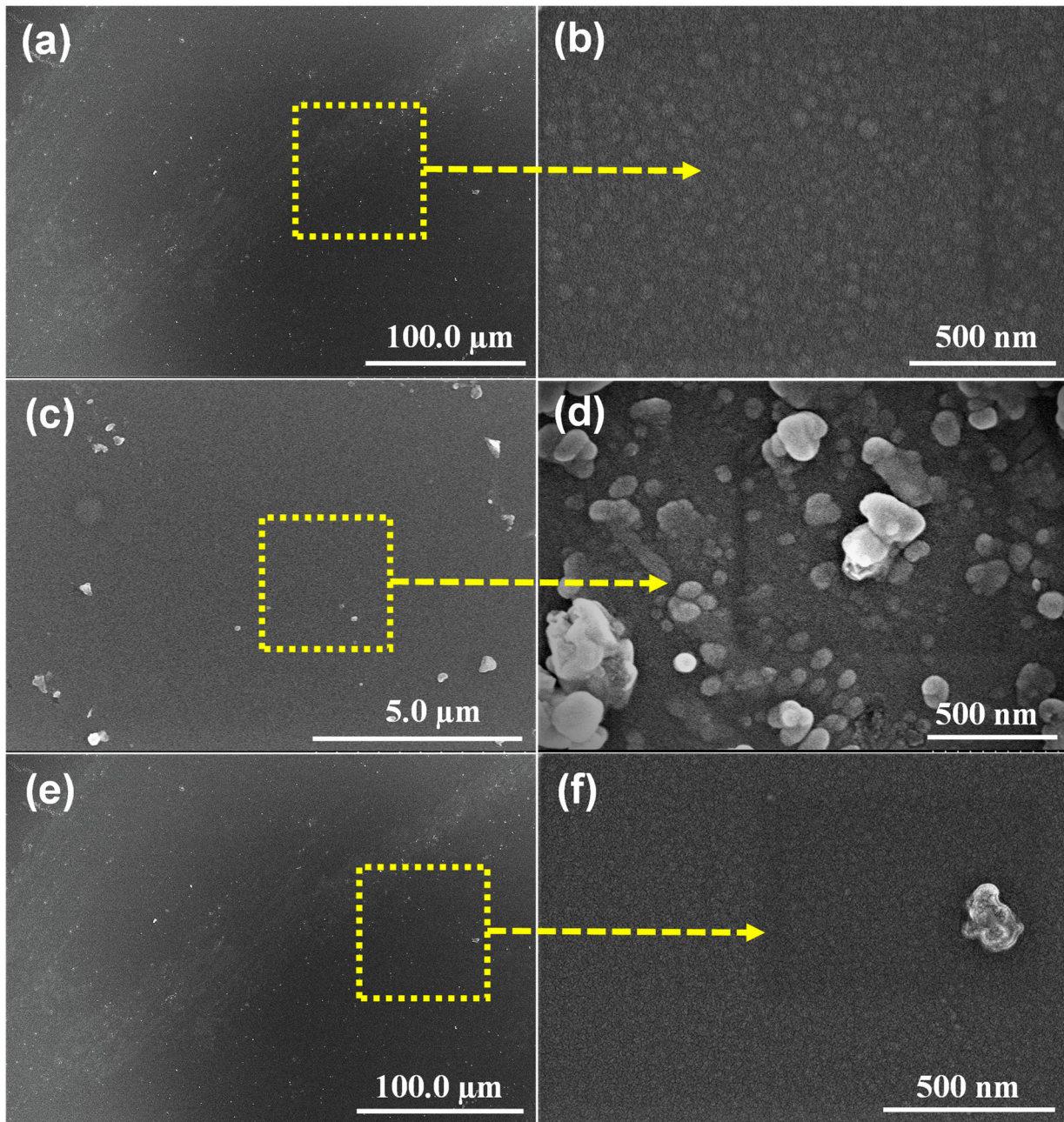


Figure 4. Scanning electron microscope micrographs of (a,b) as-deposited ZnO, (c,d) Cu-doped ZnO, and (e,f) Al-doped ZnO films at different magnifications.

Moreover, the optical properties of the as-prepared doped and undoped ZnO-based nanostructures were investigated via UV–Vis spectroscopy. The resulting optical transmittance spectra for all the three samples, viz., pure ZnO, Al-doped ZnO, and Cu-doped ZnO films, are shown in Figure 5a. All samples exhibited an average transmission of more than 80% in the visible spectrum (400–800 nm). Further, doping with both Al and Cu caused a decrease in the transmittance of the ZnO nanostructure. Additionally, the red shift seen in the transmittance spectra of the doped samples can be ascribed to the generation of hole carriers due to doping, which shifted the Fermi level towards the valence band [27,30]. We have further estimated the bandgap energy for all three samples, from the Tauc expression:

$$(\alpha h\nu) = A (h\nu - E_g)^n \quad (1)$$

where A is a proportionality constant, ν denotes the incident radiation frequency, h denotes Planck's constant, E_g is the optical bandgap of the material, and the exponent n represents the allowed transitions. By employing the above equation, it was possible to determine the optical bandgap of a material. Figure 5b plots $(\alpha h\nu)^2$ as a function of $h\nu$ (photon energy) for ZnO, Al-doped ZnO, and Cu-doped ZnO films. The bandgap values were ascertained by extrapolating the straight linear portion of the $(\alpha h\nu)^2$ versus $(h\nu)$ plot to intersect the x -axis. The estimated bandgap values for the as-deposited ZnO, Al-ZnO, and Cu-ZnO films were 3.3, 3.28, and 3.24 eV, respectively. It is noted that both Al- and Cu-doped ZnO thin films exhibited a reduction in bandgap in comparison to the pure ZnO film, which can be associated with an increase in the free carrier concentration as a result of doping [30].

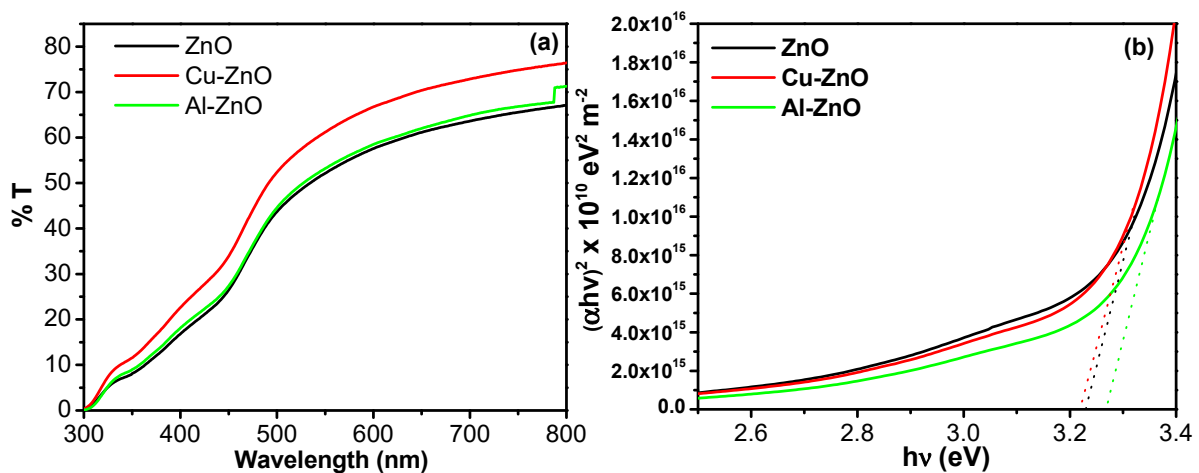


Figure 5. (a) Transmittance spectra and (b) $(\alpha h\nu)^2$ versus $h\nu$ (photon energy) plots, of pure ZnO, Al-ZnO, and Cu-ZnO.

Furthermore, Hall effect measurements were performed to analyze the electrical properties of the Al-doped and Cu-doped ZnO nanostructured films. Table 1 enlists the corresponding parameters of all the three films, such as mobility, carrier concentration, resistivity, and conductivity. It is clear from these data that the resistivity decreased following the introduction of both Al and Cu atoms into the ZnO lattice. The Cu-doped ZnO thin films demonstrated a minimum resistivity of $1.7 \times 10^{-4} \Omega \text{ cm}$, which was less than half of the resistivity of the undoped ZnO film ($4.1 \times 10^{-4} \Omega \text{ cm}$), indicating the successful incorporation of Cu atoms as dopants [30,31]. This value of resistivity is comparable to or even lower than some of the previously reported works. For example, by using a low-vacuum heat-treated target, Ghanaatshoar et al. [29] reached a resistivity of $1.8 \times 10^{-4} \Omega \text{ cm}$ in Al-doped ZnO thin films obtained using a sputtering process conducted at room temperature. Alternatively, the Cu-doped ZnO film revealed maximum conductivity ($5.8 \times 10^3 \text{ S cm}^{-1}$), which was expected due to the highest carrier concentration in this sample. Interestingly, both carrier concentration and Hall mobility increased after doping in both Al- and Cu-doped films. The highest carrier mobility was expressed by the Cu-doped ZnO film, whereas the highest Hall mobility of $16.1 \text{ cm}^2 \text{ V}^{-1} \text{ S}^{-1}$ was observed for the Al-doped ZnO nanostructure, which was higher than most values previously reported in the literature [12,31]. It is well recognized that Hall mobility demonstrates strong dependence on crystallinity, texture, grain size, and variations in grain orientations [32]. The increase in carrier concentration after doping is attributable to the substitution of host cation sites by the dopant atoms and the subsequent release of the extra electrons [31]. The slightly lower carrier concentration in Al-ZnO films in comparison to the Cu-doped films can be associated with the clustering of Al atoms and the formation of stoichiometric Al_2O_3 [33,34]. These results confirm that the Al-ZnO and Cu-ZnO films prepared using the room-temperature sputtering technique have excellent electrical properties for use in solar cell applications.

Table 1. Hall effect experimental parameters for the ZnO, Al-ZnO, and Cu-ZnO thin films.

Sample	Hall Mobility ($\text{cm}^2 \text{V}^{-1} \text{S}^{-1}$)	Carrier Concentration (cm^{-3})	Resistivity (Ωcm)	Conductivity (S cm^{-1})
ZnO	11.3	2.7×10^{20}	4.1×10^{-4}	2.4×10^3
Al-ZnO	16.1	3.5×10^{21}	3.2×10^{-4}	3.4×10^3
Cu-ZnO	13.2	4.3×10^{21}	2.04×10^{-4}	5.8×10^3

Finally, the suitability of the prepared Al-ZnO, and Cu-ZnO thin films for use as electrodes in solar cells was assessed. The fabricated solar cells were exposed to a simulated light source, and the current-voltage characteristics, short circuit current density (J_{SC}), an open circuit voltage (V_{OC}) were recorded using a source meter. Figure 6 depicts the comparative photocurrent density–voltage (J – V) characteristics of different solar cells constructed from the pure ZnO, Al-doped ZnO, and Cu-doped ZnO nanostructures. The considerable changes in J – V characteristics of the doped films vis-à-vis the pure ZnO films suggest of the Al- and Cu-doped films have enhanced photoabsorption properties. The different device parameters as estimated from the J – V characteristics, viz., J_{SC} , V_{OC} , fill factor (FF), and power conversion efficiency (η), are enumerated in Table 2. The η and FF were determined using the following relations (29):

$$\eta = (J_{SC} V_{OC} FF) / P_{in} \quad (2)$$

$$FF = (J_{max} V_{max}) / (J_{SC} V_{OC}) \quad (3)$$

where P_{in} denotes the incident light energy, and J_{max} and V_{max} are the current density and voltage, corresponding to the maximum output power in the J – V curves. From the table, it is evident that doping significantly improved the short circuit current densities of both Al-doped ZnO and Cu-doped ZnO nanostructures vis-à-vis the pristine ZnO films. Further, among the three types of photoanodes employed, the solar cells fabricated using Cu-doped ZnO exhibit a maximum photoconversion efficiency PCE of 0.56%, corresponding to short circuit current density (J_{SC}) of 4.985 mA cm^{-2} and open-circuit voltage (V_{OC}) of 0.315 V. Further, the Al-doped ZnO solar cell demonstrated an η of 0.492% with a J_{SC} of 1.539 mA cm^{-2} and a V_{OC} of 0.547 V. In comparison, undoped ZnO offered merely 0.163%, 0.762 mA cm^{-2} , and 0.533 V, respectively. Doping with either Al or Cu was found to improve the performance of ZnO-based solar cells.

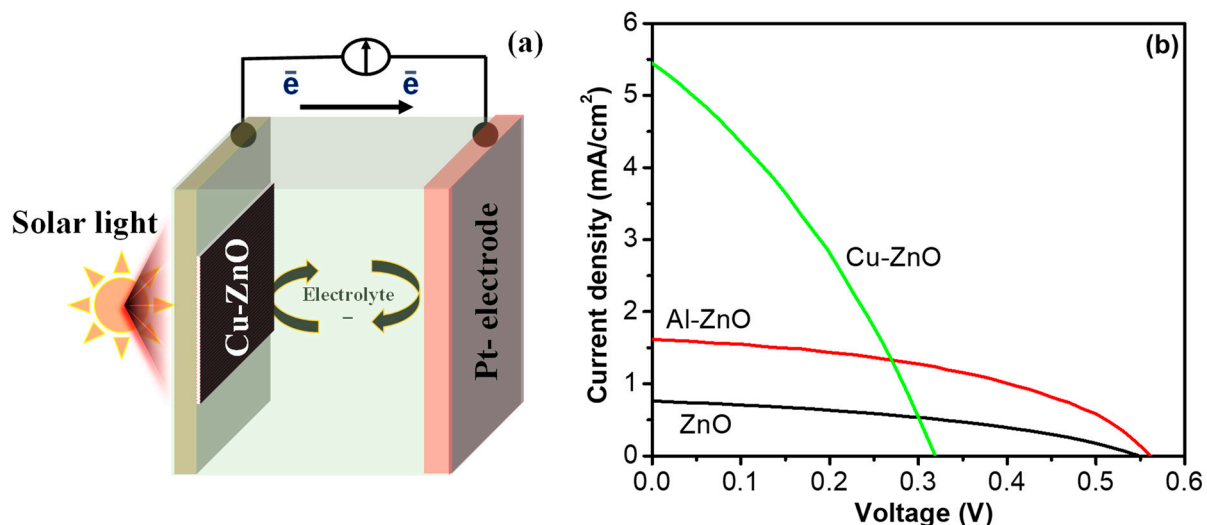
**Figure 6.** (a) Schematic diagram of prepared solar cell and (b) current density–voltage curve of the ZnO, Cu-ZnO, and Al-ZnO.

Table 2. The solar cell performance for ZnO, Cu-ZnO, and Al-ZnO.

Sample	V_{oc} (V)	J_{sc} (mA/cm ²)	PEC (%)
ZnO	0.533	0.762	0.163
Al-ZnO	0.547	1.539	0.492
Cu-ZnO	0.315	4.985	0.559

The Cu-doped ZnO material showed considerably higher photoconversion efficiency, ~4 times higher than that of the undoped ZnO photoelectrode. Moreover, the Al-doped ZnO shows ~3 times higher photoconversion efficiency than pristine ZnO. The improved performance in the case of doped solar cells is ascribable to the dopant-created trapping levels close to the conduction band of ZnO nanostructure, favoring a rapid charge transfer rate and facilitating the forward movement of low energy electrons. Consequently, the doped structures have increased photon adsorption and effective charge separation or reduced electron-hole pair (exciton) recombination, which in turn enhances the photoconversion efficiency [35].

4. Conclusions

In summary, we successfully prepared high-quality undoped ZnO, aluminum- and copper-doped ZnO thin films on FTO substrate via a facile room-temperature RF sputtering technique. The films revealed an average transmittance of ~80% in the visible region with low resistivity ($2.9 \times 10^{-4} \Omega \text{ cm}$ for Al-ZnO and $1.7 \times 10^{-4} \Omega \text{ cm}$ for Cu-ZnO) and high carrier mobility ($16.1 \text{ cm}^2 \text{ V}^{-1} \text{ S}^{-1}$ for Al-ZnO and $13.2 \text{ cm}^2 \text{ V}^{-1} \text{ S}^{-1}$ for Cu-ZnO). The low resistivity and high transmittance render these films suitable for application in transparent conductive electrodes of solar cells. Finally, the applicability of the prepared films was tested in solar cells. The Al-doped ZnO-based solar cells offered an efficiency of 0.492%, whereas the Cu-doped-ZnO-based solar cells exhibited the best performance with photocurrent of 4.985 mA cm^{-2} along with a power conversion efficiency of 0.56%, which were comparable vis-à-vis the values reported for solar cells. From these results, it can be clearly seen that the Cu-ZnO film shows the highest efficiency followed by the Al-ZnO thin film. We believe the investigations reported in this work will encourage further research activities in RF sputtered thin films for the fabrication of high-performance solar cells.

Author Contributions: M.W.A., M.Z.A., M.A. and S.A.A. did the experimental and characterization; M.W.-U.-R. and N.P. prepared the figures, data extraction revision. All the Authors contributed in writing the manuscript draft, editing and revision. All authors have read and agreed to the published version of the manuscript.

Funding: The authors acknowledge the Deanship of Scientific Research at King Faisal University for financial support under the DSR Annual Project (Grant No. 180102).

Conflicts of Interest: The authors declare no conflict of interest.

References

- Ge, Z.; Wang, C.; Chen, T.; Chen, Z.; Wang, T.; Guo, L.; Qi, G.; Liu, J. Preparation of Cu-doped ZnO nanoparticles via layered double hydroxide and application for dye-sensitized solar cells. *J. Phys. Chem. Solids* **2021**, *150*, 109833. [[CrossRef](#)]
- Kharangarh, P.; Misra, D.; Georgiou, G.E.; Chin, K.K. Evaluation of Cu back contact related deep defects in CdTe solar cells. *ECS J. Solid State Sci. Technol.* **2012**, *1*, Q110. [[CrossRef](#)]
- Sufyan, M.; Mehmood, U.; Gill, Y.Q.; Nazar, R.; Khan, A.U.H. Hydrothermally synthesize zinc oxide (ZnO) nanorods as an effective photoanode material for third-generation Dye-sensitized solar cells (DSSCs). *Mater. Lett.* **2021**, *297*, 130017. [[CrossRef](#)]
- Ringleb, A.; Ruess, R.; Hofeditz, N.; Heimbrodt, W.; Yoshida, T.; Schlettwein, D. Influence of Mg-doping on the characteristics of ZnO photoanodes in dye-sensitized solar cells. *Phys. Chem. Chem. Phys.* **2021**, *23*, 8393–8402. [[CrossRef](#)]
- Quintana, M.; Edvinsson, T.; Hagfeldt, A.A.; Boschloo, G. Comparison of dye-sensitized ZnO and TiO₂ solar cells: Studies of charge transport and carrier lifetime. *J. Phys. Chem. C* **2007**, *11*, 1035–1041. [[CrossRef](#)]

6. Zhang, Q.; Xie, C.; Zhang, S.; Wang, A.; Zhu, B.; Wang, L.; Yang, Z. Identification and pattern recognition analysis of Chinese liquors by doped nano ZnO gas sensor array. *Sens. Actuators B Chem.* **2005**, *110*, 370–376. [[CrossRef](#)]
7. Park, S.-M.; Ikegami, T.; Ebihara, K. Investigation of transparent conductive oxide Al-doped ZnO films produced by pulsed laser deposition. *Jpn. J. Appl. Phys.* **2005**, *44*, 8027. [[CrossRef](#)]
8. Jongnavakit, P.; Amornpitoksuk, P.; Suwanboon, S.; Ndiege, N. Preparation and photocatalytic activity of Cu-doped ZnO thin films prepared by the sol-gel method. *Appl. Surf. Sci.* **2012**, *258*, 8192–8198. [[CrossRef](#)]
9. Ke, Y.; Berry, J.; Parilla, P.; Zakutayev, A.; O'Hayre, R.; Ginley, D. The origin of electrical property deterioration with increasing Mg concentration in ZnMgO: Ga. *Thin Solid Films* **2012**, *520*, 3697–3702. [[CrossRef](#)]
10. Purica, M.; Budianu, E.; Rusu, E.; Danila, M.A.; Gavrila, R. Optical and structural investigation of ZnO thin films prepared by chemical vapor deposition (CVD). *Thin Solid Films* **2002**, *403*, 485–488. [[CrossRef](#)]
11. Sbrockey, N.M.; Ganesan, S. ZnO thin films by MOCVD. *III-Vs Rev.* **2004**, *17*, 23–25. [[CrossRef](#)]
12. Park, T.; Kong, B.; Cho, H.K.; Park, D.; Lee, J. Influence of gas atmosphere during growth interruption in the deposition of ZnO films by magnetron sputtering. *Phys. B Condens. Matter* **2006**, *376*, 735–740. [[CrossRef](#)]
13. Ghosh, A.; Kumari, N.; Bhattacharjee, A. Influence of Cu doping on the structural, electrical and optical properties of ZnO. *Pramana* **2015**, *84*, 621–635. [[CrossRef](#)]
14. Yang, W.; Liu, Z.; Peng, D.-L.; Zhang, F.; Huang, H.; Xie, Y.; Wu, Z. Room-temperature deposition of transparent conducting Al-doped ZnO films by RF magnetron sputtering method. *Appl. Surf. Sci.* **2009**, *255*, 5669–5673. [[CrossRef](#)]
15. Nomoto, J.-I.; Hirano, T.; Miyata, T.; Minami, T. Preparation of Al-doped ZnO transparent electrodes suitable for thin-film solar cell applications by various types of magnetron sputtering depositions. *Thin Solid Films* **2011**, *520*, 1400–1406. [[CrossRef](#)]
16. Hirahara, N.; Onwona-Agyeman, B.; Nakao, M. Preparation of Al-doped ZnO thin films as transparent conductive substrate in dye-sensitized solar cell. *Thin Solid Films* **2012**, *520*, 2123–2127. [[CrossRef](#)]
17. Sun, J.H.; Dong, S.Y.; Feng, J.L.; Yin, X.J.; Zhao, X.C. Enhanced sunlight photocatalytic performance of Sn-doped ZnO for Methylene Blue degradation. *J. Mol. Catal. A Chem.* **2011**, *335*, 145–150. [[CrossRef](#)]
18. Saputrina, T.T.; Iwantono, I.; Awitdrus, A.; Umar, A.A. Performances of dye-sensitized solar cell (DSSC) with working electrode of aluminum-doped ZnO nanorods. *Sci. Technol. Commun. J.* **2020**, *1*, 1.
19. Lee, J.H.; Song, J.T. Dependence of the electrical and optical properties on the bias voltage for ZnO: Al films deposited by rf magnetron sputtering. *Thin Solid Films* **2008**, *516*, 1377–1381. [[CrossRef](#)]
20. Wang, H.; Xu, J.; Ren, M.; Yang, L. Room temperature deposition and properties of ZnO: Al thin films by nonreactive DC magnetron sputtering. *J. Mater. Sci. Mater. Electron.* **2008**, *19*, 1135–1139. [[CrossRef](#)]
21. Lin, W.; Ma, R.; Shao, W.; Kang, B.; Wu, W. Properties of doped ZnO transparent conductive thin films deposited by RF magnetron sputtering using a series of high quality ceramic targets. *Rare Met.* **2008**, *27*, 32–35. [[CrossRef](#)]
22. Iwantono, I.; Saad, S.K.M.; Anggelina, F.; Awitdrus, A.; Ramli, M.A.; Umar, A.A. Enhanced charge transfer activity in Au nanoparticles decorated ZnO nanorods photoanode. *Phys. E Low-Dimens. Syst. Nanostruct.* **2019**, *111*, 44–50. [[CrossRef](#)]
23. Waqas Alam, M.; Khatoun, U.; Qurashi, A. Synthesis and characterization of Cu-SnO₂ nanoparticles deposited on glass using ultrasonic spray pyrolysis and their H₂S sensing properties. *Curr. Nanosci.* **2012**, *8*, 919–924. [[CrossRef](#)]
24. Park, M.S.; Min, B.I. Ferromagnetism in ZnO codoped with transition metals: Zn_{1-x}(FeCo)_xO and Zn_{1-x}(FeCu)_xO. *Phys. Rev. B* **2003**, *68*, 224436. [[CrossRef](#)]
25. Buchholz, D.B.; Chang, R.P.H.; Song, J.Y.; Ketterson, J.B. Room-temperature ferromagnetism in Cu-doped ZnO thin films. *Appl. Phys. Lett.* **2005**, *87*, 082504. [[CrossRef](#)]
26. Mohan, R.; Krishnamoorthy, K.; Kim, S.J. Enhanced photocatalytic activity of Cu-doped ZnO nanorods. *Solid State Commun.* **2012**, *152*, 375–380. [[CrossRef](#)]
27. Raja, M.; Muthukumarasamy, N.; Velauthapillai, D.; Balasundaraprabhu, R. Influence of copper on the morphology and properties of one dimensional ZnO nanorod structures. *Superlattices Microstruct.* **2014**, *72*, 102–110. [[CrossRef](#)]
28. Aravind, A.; Jayaraj, M.K.; Kumar, M.; Chandra, R. Optical and magnetic properties of copper doped ZnO nanorods prepared by hydrothermal method. *J. Mater. Sci. Mater. Electron.* **2013**, *24*, 106–112. [[CrossRef](#)]
29. Ma, Z.; Ren, F.; Ming, X.; Long, Y.; Volinsky, A.A. Cu-doped ZnO electronic structure and optical properties studied by first-principles calculations and experiments. *Materials* **2019**, *12*, 196. [[CrossRef](#)] [[PubMed](#)]
30. Chen, M.; Pei, Z.; Sun, C.; Wen, L.; Wang, X. Surface characterization of transparent conductive oxide Al-doped ZnO films. *J. Cryst. Growth* **2000**, *220*, 254–262. [[CrossRef](#)]
31. Asemi, M.; Ahmadi, M.; Ghanaatshoar, M. Preparation of highly conducting Al-doped ZnO target by vacuum heat-treatment for thin film solar cell applications. *Ceram. Int.* **2018**, *44*, 12862–12868. [[CrossRef](#)]
32. Raja, M.; Muthukumarasamy, N.; Velauthapillai, D.; Balasundaraprabhu, R.; Agilan, S.; Senthil, T.S. Quantum dot sensitized aluminium doped and copper doped ZnO nanostructure based solar cells. *J. Mater. Sci. Mater. Electron.* **2014**, *25*, 5035–5040. [[CrossRef](#)]
33. Lee, D.J.; Kim, H.M.; Kwon, J.Y.; Choi, H.; Kim, S.H.; Kim, K.B. Structural and electrical properties of atomic layer deposited Al-doped ZnO films. *Adv. Funct. Mater.* **2011**, *21*, 448–455. [[CrossRef](#)]

34. Lee, Y.M.; Lai, C.H. Preparation and characterization of solid n-TiO₂/p-NiO heterojunction electrodes for all-solid-state dye-sensitized solar cells. *Solid-State Electron.* **2009**, *53*, 1116–1125. [[CrossRef](#)]
35. Das, A.; Wary, R.R.; Nair, R.G. Cu modified ZnO nanoflakes: An efficient visible light-driven photocatalyst and a promising photoanode for dye sensitized solar cell (DSSC). *Solid State Sci.* **2020**, *104*, 106290. [[CrossRef](#)]